Biased G Protein-Independent Signaling of Dopamine D_1-D_3 Receptor Heteromers in the Nucleus Accumbens

Xavier Guitart[1] · Estefanía Moreno[2] · William Rea[1] · Marta Sánchez-Soto[1] · Ning-Sheng Cai[1] · César Quiroz[1] · Vivek Kumar[3] · Liam Bourque[1] · Antoni Cortés[2] · Enric I. Canela[2] · Christopher Bishop[4] · Amy H. Newman[3] · Vicent Casadó[2] · Sergi Ferré[1] (ORCID)

Abstract

Several studies found in vitro evidence for heteromerization of dopamine D_1 receptors (D1R) and D_3 receptors (D3R), and it has been postulated that functional D1R-D3R heteromers that are normally present in the ventral striatum mediate synergistic locomotor-activating effects of D1R and D3R agonists in rodents. Based also on results obtained in vitro, with mammalian transfected cells, it has been hypothesized that those behavioral effects depend on a D1R-D3R heteromer-mediated G protein-independent signaling. Here, we demonstrate the presence on D1R-D3R heteromers in the mouse ventral striatum by using a synthetic peptide that selectively destabilizes D1R-D3R heteromers. Parallel locomotor activity and ex vivo experiments in reserpinized mice and in vitro experiments in D1R-D3R mammalian transfected cells were performed to dissect the signaling mechanisms of D1R-D3R heteromers. Co-administration of D1R and D3R agonists in reserpinized mice produced synergistic locomotor activation and a selective synergistic AKT phosphorylation in the most ventromedial region of the striatum in the shell of the nucleus accumbens. Application of the destabilizing peptide in transfected cells and in the shell of the nucleus accumbens allowed demonstrating that both in vitro and in vivo co-activation of D3R induces a switch from G protein-dependent to G protein-independent D1R-mediated signaling determined by D1R-D3R heteromerization. The results therefore demonstrate that a biased G protein-independent signaling of D1R-D3R heteromers localized in the shell of the nucleus accumbens mediate the locomotor synergistic effects of D1R and D3R agonists in reserpinized mice.

Keywords GPCR heteromers · Dopamine D_1 receptor · Dopamine D_3 receptor · Reserpine · Functional selectivity

---

Xavier Guitart and Estefanía Moreno contributed equally to this work.

✉ Vicent Casadó
vcasado@ub.edu

✉ Sergi Ferré
sferre@intra.nida.nih.gov

[1] Integrative Neurobiology Section, National Institute on Drug Abuse, Intramural Research Program, National Institutes of Health, Baltimore, MD 21224, USA

[2] Department of Biochemistry and Molecular Biomedicine of the Faculty of Biology and Institute of Biomedicine of the University of Barcelona and Center for Biomedical Research in Neurodegenerative Diseases Network, 08028 Barcelona, Spain

[3] Medicinal Chemistry Section, National Institute on Drug Abuse, Intramural Research Program, National Institutes of Health, Baltimore, MD 21224, USA

[4] Behavioral Neuroscience Program, Department of Psychology, Binghamton University, Binghamton, NY 13902, USA

Introduction

The main localization of dopamine D_3 receptors is the most ventromedial region of the striatum, in the shell of the nucleus accumbens (NAc) and the olfactory tubercle [1, 2], where they are predominantly expressed in GABAergic efferent neurons expressing D_1 receptors (D1R) [1, 3]. Several studies found in vitro evidence for heteromerization of D1R and D3R [4–6], and it has been postulated that functional D1R-D3R heteromers are present in the ventromedial striatum and involved, not only with the pharmacological effects of D3R ligands but also with the pathogenesis of several neuropsychiatric disorders, including L-DOPA-induced dyskinesia and substance use disorders (see "Discussion" and [7–9]).

It is very well established that locomotor activity induced by dopamine receptor agonists in reserpinized mice represents activation of striatal post-synaptic receptors, without the confounding effect of endogenous dopamine. Therefore, by using

different dopamine receptor agonists, this classical model allows to dissect the role of the different striatal post-synaptic dopamine receptor subtypes on the modulation of locomotor activity [10, 11]. It was initially shown in reserpinized mice that a D3R agonist does not produce locomotor activation, but that it significantly potentiates the locomotor activation induced by a D1R agonist [6]. However, D1R and D3R couple respectively to Gs/olf and Gi/o proteins [12]. We should then expect an antagonistic effect upon simultaneous activation of both receptors, based on a canonical Gs-Gi antagonistic interaction at the adenylyl cyclase (AC) level, by which a Gi-coupled receptor inhibits a Gs-coupled receptor-mediated AC activation [13]. Results obtained by Fiorentini et al. [4] suggested that within the D1R-D3R heteromer, D3R activation potentiates D1R-mediated AC signaling. However, more recently, the canonical Gs-Gi antagonistic interaction could be demonstrated in cells expressing D1R-D3R heteromers and co-transfected with the predominant striatal AC subtype (AC5) [5]. Nevertheless, a concomitant synergistic interaction between D1R and D3R agonists could be demonstrated with β-arrestin recruitment and at the MAPK signaling level, which was mediated by a G protein-independent mechanism. Thus, MAPK activation induced by the simultaneous application of D1R and D3R agonists was not counteracted by incubation with pertussis toxin [5]. This interaction was indeed shown to be dependent on D1R-D3R heteromerization, since it was counteracted by synthetic peptides that specifically destabilize the D1R-D3R heteromer [5]. It was therefore hypothesized that the synergistic locomotor-activating effect of D1R and D3R agonists in reserpinized mice is mediated by a G protein-independent synergistic effect determined by D1R-D3R heteromers localized in the ventromedial striatum. However, unequivocal demonstration of direct intermolecular interactions in situ of the existence of D1R-D3R heteromers in the brain still remained to be established. The goal of the present study was to demonstrate that G protein-independent D1R-D3R-mediated signaling in the ventromedial striatum mediates the locomotor synergistic effects of D1R and D3R agonists in reserpinized mice.

Material and Methods

Cell Culture and Transfection

CHO cells and stably transfected HEK-293T cells (D3R and D1R-D3R clones) were grown in Dulbecco's modified Eagle's medium (DMEM; Gibco, Paisley, Scotland) supplemented with 2-mM L-glutamine, 100-U/ml penicillin/streptomycin, 100-μg/ml sodium pyruvate, minimum essential medium nonessential amino acid solution (1/100), and 5% (*v/v*) heat-inactivated fetal bovine serum (FBS; Invitrogen, Carlsbad, CA). For cell clones, the corresponding selection antibiotic was added in the culture medium (300-μg/ml

hygromicin B). Cells were maintained at 37 °C in an atmosphere of 5% CO_2. HEK-239 and CHO cells growing in 6-well dishes were transiently transfected with the corresponding fusion protein cDNA (indicated in the corresponding figure legend) by the PEI method, as described in detail elsewhere [14]. Sample protein concentration was determined using a Bradford assay kit (Bio-Rad, Munich, Germany) and bovine serum albumin dilutions as standards.

HIV TAT Fused-TM Peptides

Peptides, with the amino acid sequence of transmembrane domains (TMs) of the D1R, were used as heteromer-destabilizing agents [5, 15–18]. To allow intracellular delivery, a peptide can be fused to the cell-penetrating HIV trans-activator of transcription (TAT) peptide (YGRKKRRQRRR) [19]. HIV TAT fused to a TM peptide can be inserted effectively into the plasma membrane as result of both the penetration capacity of the TAT peptide and the hydrophobic property of the TM peptide [16]. To obtain the right orientation of the inserted peptide respect to the receptor, HIV TAT peptide was fused to the C-terminus of peptides with the amino acid sequence of TM 5, TM 6, and TM 7 of D1R (TM5, TM6, and TM7 peptides, respectively). The peptides were synthesized by Genemed Synthesis, Inc. (San Antonio, TX). Their sequences were as follows: TM5, TYAISSSLISFYIPVAIMIVTYTSIYYGRKKRRQRRR; TM6, YGRKKRRQRRRTLSVIMGVFVCCWL PFFISNCMVPFCG; TM7, FDVFVWFGWANSSLNP IIYAFNADFYGRKKRRQRRR.

cAMP Accumulation

Homogeneous time-resolved fluorescence energy transfer (HTRF) assays were performed using the Lance Ultra cAMP kit (PerkinElmer, Waltham, MA), based on competitive displacement of a europium chelate-labeled cAMP tracer bound to a specific antibody conjugated to acceptor beads. The optimal cell density for an appropriate fluorescent signal was first established by measuring the TR-FRET signal determined as a function of forskolin concentration using different cell densities. Forskolin dose-response curves were related to the cAMP standard curve in order to establish a cell density with a response covering most of the dynamic range of the cAMP standard curve. Cells were not treated or treated with vehicle or 4 μM of the indicated TM peptides for 4 h at 37 °C in an atmosphere of 5% CO_2. Cells were then grown (800 cells/ well) in white ProxiPlate 384-well microplates (PerkinElmer, Waltham, MA) in medium containing 50-μM zardaverine, stimulated with agonists for 10 min before adding 0.5-μM forskolin or vehicle and incubated for an additional 15-min period. Fluorescence at 665 nm was analyzed on a PHERAstar Flagship microplate reader equipped with an

HTRF optical module (BMG Lab Technologies, Offenburg, Germany).

Phosphorylation of ERK1/2 and AKT

D1R and D1-D3R HEK293T cell lines were maintained in culture as described above. Cells were seeded to 12-well plates (0.25×10^6/well) in full growth medium. The day before the assay, the medium was changed to DMEM with no FBS for approximately 16 h before the addition of ligands. Cells were then incubated or not with the selective D3R antagonist VK4–116 or the non-selective D_2-like receptor antagonist eticlopride for 10 min and then with the D3R agonist PD 128907 for 15 min. Cells were then rinsed with ice-cold phosphate-buffered saline and lysed by the addition of 100 μl of ice-cold lysis buffer (provided by the commercial kit; Cell Signaling Technology, Danvers, MA). Determination of pMAPK levels was performed using an enzyme-linked sandwich ELISA kit (Cell Signaling Technology) following the protocol indicated by the provider. Transfected CHO cells were cultured in serum-free medium for 16 h before the addition of any agent and were not treated or treated with the PKA inhibitor H-89 (10 μM; Tocris, Pittsburgh, PA) for 30 min at 37 °C. Then, cells were not incubated or incubated with the indicated antagonist for 15 min at 37 °C and activated for 7 min with the indicated agonist. Cells were rinsed with ice-cold phosphate-buffered saline and lysed by the addition of 500 μl of ice-cold lysis buffer (50-mM Tris-HCl pH 7.4, 50-mM NaF, 150-mM NaCl, 45-mM β-glycerophosphate, 1% Triton X-100, 20-μM phenyl-arsine oxide, 0.4-mM NaVO₄, and protease inhibitor cocktail). The cellular debris was removed by centrifugation at 13,000 ×g for 5 min at 4 °C, and the protein was quantified by the bicinchoninic acid method using bovine serum albumin dilutions as standard. To determine the level of phosphorylated proteins, equivalent amounts of protein (10 μg) were separated by electrophoresis on a denaturing 7.5% SDS-polyacrylamide gel and transferred onto PVDF-FL membranes by Western blot. Odyssey blocking buffer (LI-COR Biosciences, Lincoln, NE) was then added, and the membrane was rocked for 90 min. The membranes were then probed for 2–3 h with a mixture of a mouse anti-phospho-ERK1/2 antibody (1:2500, Sigma-Aldrich, St. Louis, MO) and rabbit anti-ERK1/2 antibody that recognizes both phosphorylated and non-phosphorylated ERK1/2 (1:40000, Sigma-Aldrich) to quantify phospho-ERK1/2 or a rabbit anti-phospho-Ser473-AKT antibody (1:2500; SAB Signalway Antibody, College Park, MD) and a mouse anti-total-AKT antibody (1:2500; Cell Signaling Technology) to quantify phospho-AKT. Bands were visualized by the addition of a mixture of IRDye 800 (anti-mouse) antibody (1:10000, Sigma-Aldrich) and IRDye 680 (anti-rabbit) antibody (1:10000, Sigma-Aldrich) for 1 h and scanned by the Odyssey infrared scanner (LI-COR Biosciences, Lincoln,

NE). Band densities were quantified using the scanner software, exported to Excel (Microsoft, Redmond, WA). The level of phosphorylated proteins was normalized for differences in loading using the total (phosphorylated plus non-phosphorylated) protein band intensities.

β-Arrestin Recruitment

β-Arrestin-1 recruitment was determined by Bioluminescence Resonance Energy Technique (BRET) experiments in CHO cells 48 h after transfection with the indicated amounts of cDNA corresponding to D1R, D3R-YFP, and β-arrestin-1-Rluc. Cells (20-mg total protein from a cell suspension per well in 96-well microplates) were not treated or treated for 10 min with the indicated antagonists, and 5-μM coelenterazine H was added before stimulation with the agonist for 7 min. BRET readings were collected using a Mithras LB 940 (Berthold Technologies, Oak Ridge, TN) that allows the integration of the signals detected in the short-wavelength filter at 485 nm (440–500 nm) and the long-wavelength filter at 530 nm (510–590 nm). The net BRET is defined as [(long-wavelength emission) / (short-wavelength emission)] − Cf, where Cf corresponds to [(long-wavelength emission) / (short-wavelength emission)] for the donor construct expressed alone in the same experiment. BRET is expressed as milli-BRET units (net BRET × 1000).

Locomotor Activity in Reserpinized Mice

Male Swiss Webster mice (Charles River Laboratories, Wilmington, MA), experimentally naïve at the start of the study and weighing 20–25 g, were used. All animals used in this study were maintained in accordance with the National Institutes of Health Guide for the Care and use of Laboratory Animals, and the animal research conducted to perform our study was reviewed and approved by the National Institute on Drug Abuse Intramural Program Animal Care and Use Committee (protocol # 15-BNRB-73). Reserpine (Tocris) was dissolved in a drop of glacial acetic acid and made up to volume with 5.5% glucose and administered subcutaneously. The dose of reserpine (5 mg/kg) has been previously shown to produce pronounced striatal dopamine depletion in mice (more than 95% depletion) [11]. Mice were reserpinized 20 h prior to the start of the locomotor activity recording. The drugs to be tested were prepared in sterile saline and administered intraperitoneally. The volume of injection was 10 ml/kg for all drugs. All drugs were from Tocris, except VK4–116, (N-(4-(4-(3-chloro-5-ethyl-2-methoxyphenyl)piperazin-1-yl)-3-hydroxybutyl)-1H-indole-2-carboxamide oxalate), which was synthesized at NIDA IRP according to the published procedure (compound 19 in Kumar et al. [20]. Locomotor activity was recorded immediately after the animals were introduced in the open field after the

administration of the agonists. Antagonists were administered 15 min before the agonists. All values registered per 10 min were transformed (square root; see rationale below, in the "Statistical Analysis" section), and the average of the results obtained from the 10 min-periods recorded for 1 h was used for calculations.

Surgery, Intracerebral Infusion, and Ex Vivo Immunohistochemistry in Reserpinized Mice

On day one, equithesin (4.44 g of chloral hydrate, 0.972 g of Na pentobarbital, 2.124 g of $MgSO_4$, 44.4 ml of propylene glycol, 12 ml of ethanol, and distilled water up to 100 ml of the final solution; NIDA IRP Pharmacy) was administered to mice to induce anesthesia (3 ml/kg), and a thin silica tube (outer diameter, 105 μm) was implanted unilaterally in the NAc shell (coordinates in millimeters from bregma, with a 10° angle in the coronal plane: anterior, 1.1; lateral, 0.75; dorso-ventral, − 4.5). After surgery, mice were allowed to recover for 20 h and on day two were reserpinized (reserpine, 5 mg/kg, subcutaneously). Intracerebral infusion experiments of TAT-TM peptides (TM5 or TM7 of the D1R) or the PKA inhibitor H-89 were performed on the third day on freely moving mice. TAT-TM peptides were dissolved in 0.1% DMSO in artificial cerebrospinal fluid to a final concentration of 60 μM. H-89 was dissolved in artificial cerebrospinal fluid to a final concentration of 100 μM. Peptides and H-89 were injected with a 1-μl syringe driven by an infusion pump and connected to the implanted silica tube and intracranially delivered at a rate of 16.6 nl/min for 60 min. The agonists were systemically (i.p.) administered 40 min after the beginning of the 60-min period of intracranial infusion. After 60 min of intracranial infusion (20 min after the agonists administration), the animals were given an overdose of equitesin and perfused transcardially with 0.1-M phosphate-buffered saline (PBS) followed by ice-cold 4% paraformaldehyde in PBS delivered with a peristaltic pump at 20 ml/min for 5 min. Brains were extracted and post-fixed overnight in the same fixative and stored in a 30% sucrose solution for at least 48 h at 4 °C. Coronal sections (40-μm thick) were cut in a cryostat (model CM3050S, Leica) and collected in PBS. Sections were then first incubated for 15 min with PBS with 0.2% Triton X-100 and then were incubated with PBS containing 0.1% Triton X-100 and 3% BSA. After rinsing the slices three times with PBS, the sections were incubated overnight with the primary antibody (phospho-ERK1/2, 1:400; phospho-AKT, 1:300, Cell Signaling Technology) at 4 °C. On day two, after three rinses in PBS, sections were incubated for 2 h at room temperature with the anti-rabbit Cy5-conjugated antibody (1:250, GE Health Care, Little Chalfont Buckinghamshire, UK).

Finally, after three rinses with PBS, brain slices were mounted under coverslips using Prolong Diamond Antifade Mountant (Invitrogen, Carlsbad, CA) for fluorescent confocal microscopic examination. Confocal fluorescence microscopy images were acquired with a confocal microscope (Examiner Z1, Zeiss, Gottingen, Germany) with a laser scanning module (LSM-710, Zeiss). Positive cells/mm^2 was counted within the area of the shell of the NAc from several coronal sections immediately anterior to the cannula implantation (from 2.28 to 1.44 mm anterior to bregma).
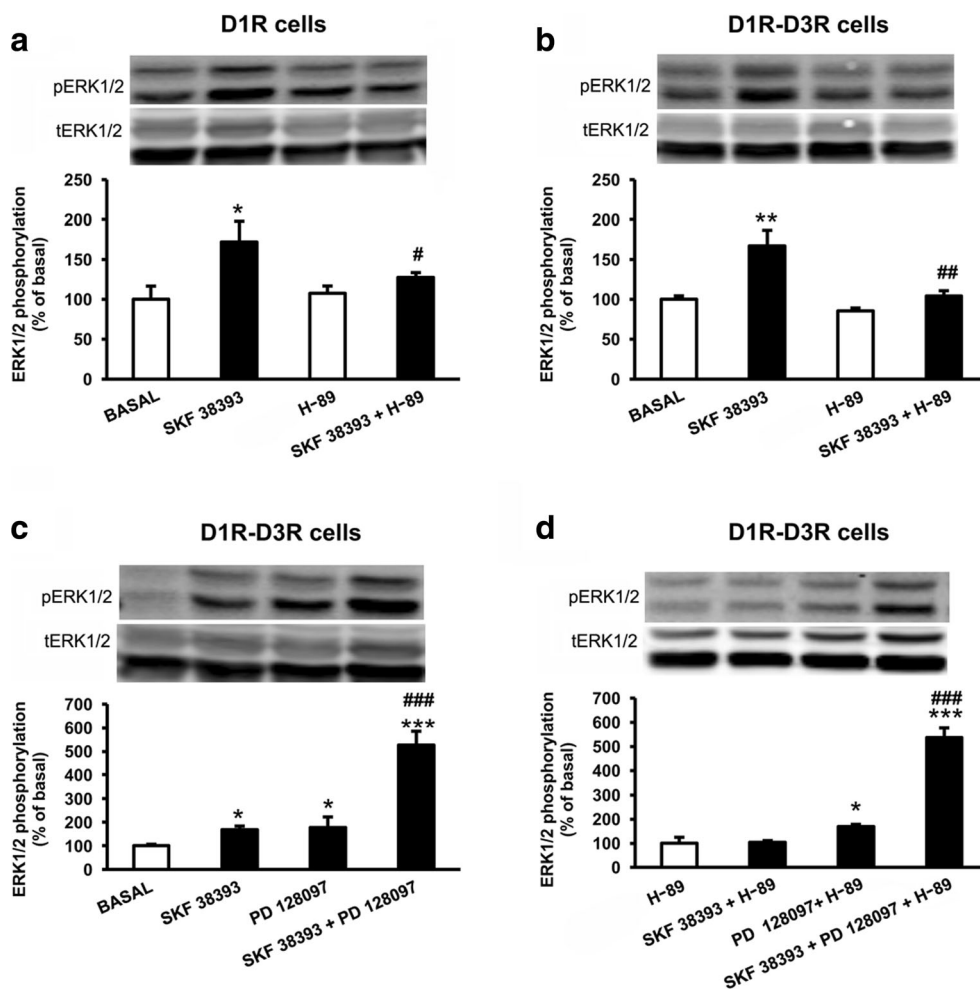
q-PCR in Reserpinized Mice

Twenty hours after administration of reserpine, mice were given an overdose of equitesin, the brains removed, and the striata dissected out and separated in dorsal and ventral striatum (region including NAc shell and core and olfactory tubercle). Tissues were homogenized by sonication, and total RNA was extracted using RNeasy® Plus Mini kit (Qiagen, Hilden Germany). Total RNA was converted to cDNA by RNA to cDNA EcoDry (Takara Bio USA, Mountain View, CA) using Oligo-dt primer. Quantitative real-time RT-PCR (q-PCR) was performed and analyzed using LightCycler instrument 480 II (Roche, Basel Switzerland). PCR reactions were done in a total volume of 20 μl in PCR mix containing 10-μl 2× LightCycler probe master, 500-nM reference gene primer (GAPDH), 500 nM of each sense and antisense primer, 100 nM of each target gene probe and reference gene probe, and 5 μl of 100 ng cDNA, adding DEPC-treated H_2O to a total volume of 20 μl. Normalization of sample cDNA content was performed using the comparative threshold (ΔΔCT) cycle method, in which the number of target gene copies was normalized to an endogenous reference gene, GAPDH. CT was defined as the fractional cycle number at which the fluorescence generated by probe cleavage passes a fixed threshold baseline when amplification of the PCR product is first detected. The primers and probes were designed using Universal Probe Library Assay Design Center (Roche). Primer sequences and probes are as follows: D1R-F and D1R-R, tctggtttacctgatccctca and gcctcctccctcttcaggt; D3R-F and D3R-R, accctggatgtcatgatgtg and ggcatgaccactgctgtgta; GADPH-F and GADPH-R, atggtgaaggtcggtgtga and aatctccactttgccactgc.

Statistical Analysis

One-way ANOVA followed by Newman-Keuls post hoc comparisons was used for all the in vitro (ERK1/2 and AKT phosphorylation, cAMP formation and β-arrestin recruitment), ex vivo experiments with AKT phosphorylation,

and in vivo experiments (locomotion). Dose-response inhibition curves of the counteracting effect of VK4–116 and eticlopride on PD 128907-mediated inhibition of forskolin-induced cAMP and on PD 128907-mediated ß-arrestin recruitment were obtained by non-linear regression analysis with least squares fit to determine IC50 (concentration of an inhibitor where the response is reduced by half) and Emax (maximal inhibitory effect) values. A paired t test was applied for statistical comparisons of the values of ERK1/2 phosphorylation from the NAc ipsilateral to the cannula implantation versus the contralateral NAc to control the substantial interindividual variability of ERK1/2 phosphorylation induced by the dopamine receptor agonists (see "Results"). No statistical method was used to predetermine sample sizes, which were based on previous studies [5, 6, 21]. The square root transformation of the locomotion data was applied to reduce the asymmetric statistical distribution of the recorded raw data (skewness to the right) and decrease significant differences in the variances between differently treated groups [22]. Prism 7 (GraphPad Software, San Diego CA) was used to carry out all statistical analyses, non-linear regression analysis, and graphics.

Results

D3R Activation in the D1R-D3R Heteromer Switches D1R-Mediated MAPK Activation from a G Protein Dependent to a G Protein Independent Mechanism in Transfected Cells

We previously reported evidence indicating that in mammalian transfected cells, activation of D3R produces MAPK activation by a G protein-independent mechanism, since it could not be blocked by pertussis toxin [5]. On the other hand, previous studies had shown evidence for a predominant Gs/olf-dependent mechanism of striatal D1R-mediated MAPK activation [23]. In agreement, in CHO cells transiently transfected with D1R or with D1R and D3R, the protein kinase A (PKA) inhibitor H-89 completely blocked ERK1/2 phosphorylation induced by the D1R agonist SKF 38393 (Fig. 1a, b), but not by the D3R agonist PD 128907 [6] (Fig. 1c, d). As previously reported [5], co-administration of the D1R and D3R agonists produced a synergistic effect on ERK1/2 phosphorylation, but this was not modified by H-89 (Fig. 1c, d). The results indicate that irrespective of the

Fig. 1 Effect of the PKA inhibitor H-89 on agonist-induced ERK1/2 phosphorylation in D1R and D1R-D3R cells. ERK1/2 phosphorylation in CHO cells transfected with D1R-Rluc cDNA (1-µg cDNA) alone (**a**) or D1R-Rluc (1-µg cDNA) and D3R-YFP (1.3-µg cDNA) (**b**–**d**). In 48 h post-transfection, D1R or D1R-D3R cells were pre-treated or not with the PKA inhibitor H-89 (10 µM for 30 min) and were treated for 7 min with the D1R agonist SKF 38393 (1 µM) (**a**–**d**), the D3R agonist PD 128907 (1 µM) (**c**–**d**) or both (**c**–**d**). Quantification of phosphorylated ERK1/2 was determined by Western blot. Representative blots are shown. Values are mean ± S.E.M. ($n = 4$ with duplicates) and are expressed as percentage of basal or non-treated cells; *, **, and ***: $p < 0.05$, $p < 0.01$, and $p < 0.001$ versus basal; #, ##, and ###: $p < 0.05$, $p < 0.01$, and $p < 0.001$ versus SKF 38393 (one-way ANOVA followed by Newman-Keuls post hoc comparisons)

presence of D3R, D1R activation induces a predominant G protein-dependent MAPK activation, while co-activation of D3R in the D1R-D3R heteromer determines a predominant G protein-independent MAPK activation. The D3R-dependent switch of D1R signaling from a G protein-dependent to a G protein-independent mechanism would involve the silencing of the D1R-mediated G protein-dependent signaling by means of the canonical Gs-Gi antagonistic interaction at AC. Hence, we could reproduce the canonical interaction with cAMP experiments and demonstrate that it depends on D1R-D3R heteromerization. In D1R-D3R transiently transfected CHO cells, both forskolin and SKF 38393 produced cAMP accumulation, which was counteracted by the D3R agonist 7-OH-PIPAT (Fig. 2a). Then, the ability of the D3R agonist to counteract cAMP formation induced by SKF 38393, but not by forskolin, was selectively blocked by the application of D1R-D3R heteromer-interfering peptides (with the amino acid sequence of TM 5 or TM 6 of the D1R, TM5, and TM6 peptides; but not with the control peptide TM7 of D1R) (Fig. 2b–d) [5]. These results imply that in the D1R-D3R heteromer, D3R co-activation blunts D1R-mediated G protein-dependent signaling. But, they would also imply that the synergistic effect of D1R and D3R agonists on MAPK

activation depends on a D3R-mediated G protein-independent signaling and a D3R-mediated G protein-independent D1R biased signaling. In fact, in vivo, this should be the only mechanism of operation by the endogenous neurotransmitter, dopamine, since it has significantly higher affinity for D3R than for D1R [24].

Using our previously characterized D3R and D1R-D3R HEK-293T cell lines [5], we evaluated the effect of different antagonists on their ability to counteract the ability of the D3R agonist PD 128907 (1 μM) to induced MAPK activation. Unexpectedly, in both cell lines, the recently reported selective D3R antagonist VK4–116 [20] was much less potent than the non-selective D_2-like receptor antagonist eticlopride, only being able to significantly reduce the effect of the D3R agonist at submicromolar concentrations (Fig. 3a–d), while their respective in vitro affinities for D3R were in the nanomolar-subnanomolar range [25]. Anticipating a functional selectivity of VK4–116, we also compared the ability of both antagonists to counteract the effect of PD 128907 on forskolin-induced cAMP accumulation and on β-arrestin recruitment in CHO cells transiently transfected with D1R and D3R. Figure 4 shows dose-response inhibition curves of the counteracting effect of VK4–116 and eticlopride on PD 128907-mediated

Fig. 2 Effect of D1R TAT-TM peptides on adenylyl cyclase signaling in D1R-D3R cells. In a–d, CHO cells were transfected with the cDNA corresponding to D1R-Rluc (1-μg cDNA) and D3R-YFP (1.5-μg cDNA). In 48 h post-transfection, D1R-D3R cells were pre-treated for 4 h with vehicle (a) or with 4 μM of D1R TM5 (b), D1R TM6 (c), or TM7 (d) peptides. Cells were treated for 7 min with medium, the D1R agonist SKF 38393 (1 μM), the D3R agonist 7-OH-PIPAT (1 μM), or both in the absence or in the presence of 0.5-μM forskolin (FK) for 15 min. Values of cAMP accumulation are shown as mean ± S.E.M. ($n = 4$ with duplicates) and expressed as percentage of FK-treated cells in each condition (100% represents 80–100-pmols cAMP/10^6 cells); *** $p < 0.001$ versus basal; ### $p < 0.001$ versus FK; &&& $p < 0.001$ versus SKF 38393, respectively (one-way ANOVA followed by Newman-Keuls post hoc comparisons)
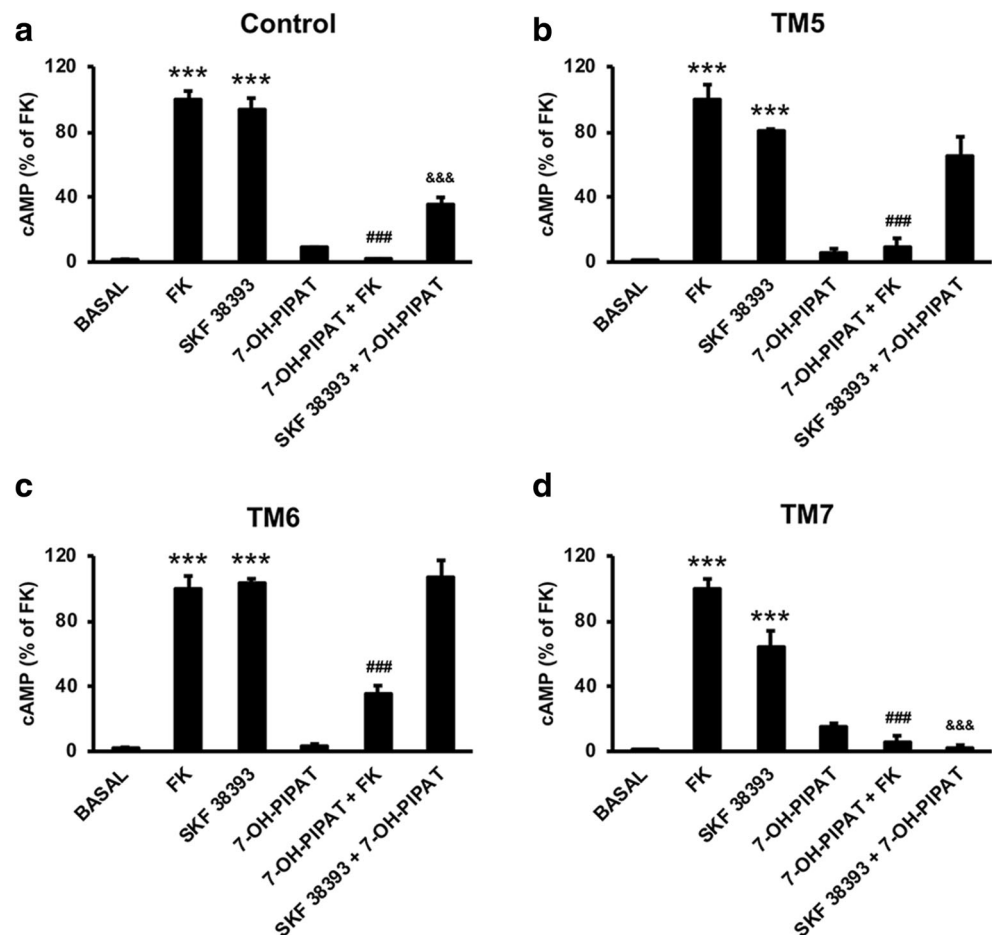
Fig. 3 Differential effect of the D3R antagonists VK4–116 and eticlopride on agonist-induced ERK1/2 phosphorylation in D3R and D1R-D3R cells. HEK-293T cell lines stably trasfected with D3R (**a**, **c**) and D1R and D3R (**b**, **d**), previously described and characterized [5], were treated with for 10 min with vehicle or with the D3R antagonist VK4–116 (**a**, **b**) (0–3 μM) or the D₂-like receptor antagonist eticlopride (**c**, **d**) (0–30 nM) before treatment for 7 min with medium or the D3R agonist PD 128907 (1 μM) for 15 min. Quantification of phosphorylated ERK1/2 was determined by ELISA. Values are mean ± S.E.M. ($n = 7$–9 with duplicates) and are expressed as % of basal; *, **, and *** $p < 0.05$, $p < 0.01$, and $p < 0.001$ versus 0 nM of VK4–116 (one-way ANOVA followed Newman-Keuls post hoc comparisons)
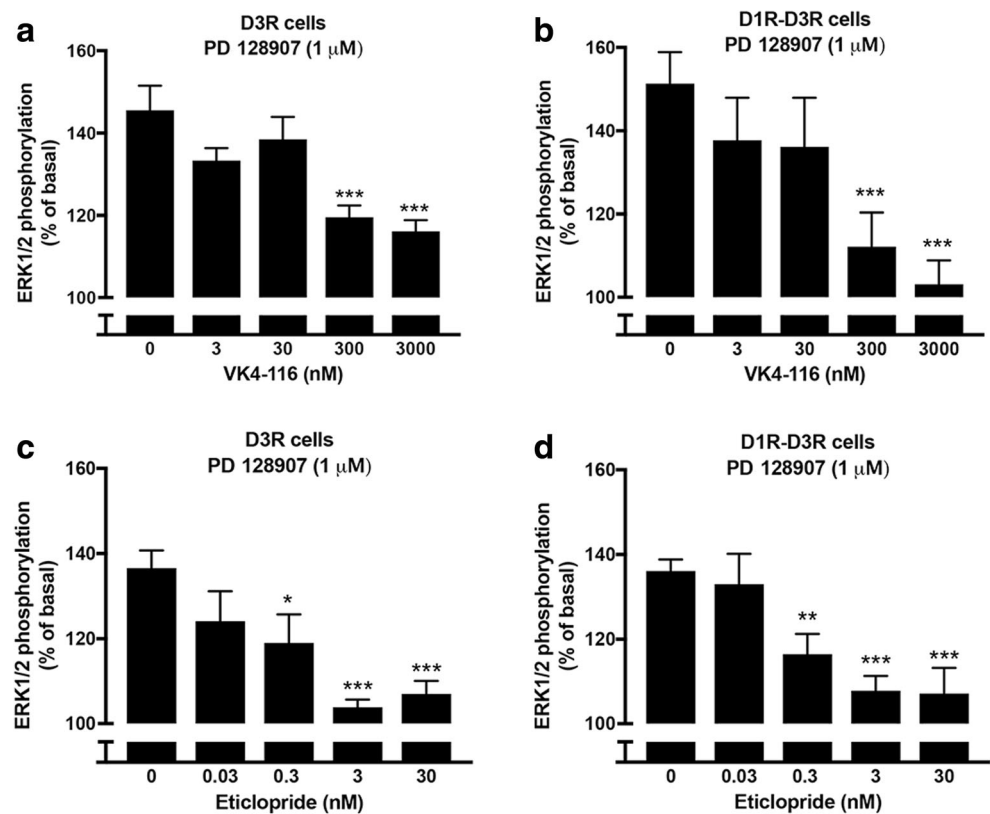
inhibition of forskolin-induced cAMP and on PD 128907-mediated ß-arrestin recruitment. A non-linear regression analysis with least squares fit showed similar IC50 and Emax values for VK4–116 and eticlopride on PD 128907-mediated inhibition of forskolin-induced cAMP (0.19 and 0.41 nM and 74.2 and 81.5%, respectively). On β-arrestin recruitment, on the other hand, VK4–116 was about 10 times less potent than eticlopride (IC50 values: 0.3 and 0.04 nM, respectively) and showed a partial antagonistic effect, as compared with the full antagonism of eticlopride (Emax values: 46.3 and 95.1%, respectively). Therefore, VK4–116 represents a biased antagonist with significantly higher potency and efficacy at blocking G protein-dependent than independent D3R signaling, providing a pharmacological tool to dissect G protein-dependent and independent D3R signaling in vivo.

D3R Activation in the D1R-D3R Heteromer Switches D1R-Mediated MAPK Activation from a G Protein Dependent to a G Protein Independent Mechanism in the NAc Shell of Reserpinized Mice

With these pharmacological findings in cells, we could address our goal of demonstrating pharmacologically significant D1R-D3R heteromers in the mouse ventromedial striatum and its involvement in the D1R-D3R synergy at the behavioral level. It is very well established that locomotor activity

induced by dopamine receptor agonists in reserpinized mice represents activation of striatal post-synaptic receptors, without the confounding effect of endogenous dopamine. Therefore, by using different dopamine receptor agonists, this classical model allows to dissect the role of the different striatal post-synaptic dopamine receptor subtypes on the modulation of locomotor activity [10, 11]. We first determined selective doses of D1R and D3R ligands in the reserpinized mice (20 h after reserpinization). In a recently reported study using the same model, we showed that the D1R full agonist SKF 81297 produces a dose-dependent increase in locomotor activation, with an ED50 of about 5 mg/kg [21]. The effect of SKF 81297 was counteracted with the D1R antagonist SCH 23390 (0.5 mg/kg) but not by eticlopride, at a dose (0.5 mg/kg) that did not counteract locomotor activation induced by the D2R-D3R-D4R agonist quinpirole [21]. Here, we reproduced the same results of SKF 81297 alone (5 mg/kg), its counteraction with SCH 23390 (0.5 mg/kg), lack of counteraction with eticlopride (0.3 mg/kg), and lack of counteraction with VK4–116 (up to 100 mg/kg) (Fig. 5a). As previously reported [6], at the dose of 1 mg/kg, PD 128907 did not produce locomotor activation but significantly increased the locomotor activation of a D1R agonist, SKF 81297 (5 mg/kg) (Fig. 5b). The dependence on D3R activation of PD 128907 (1 mg/kg) was also previously demonstrated in D3R KO mice [6]. Therefore, in the reserpinized mice model, locomotor activity induced by SKF 81297 (5 mg/kg) represents selective
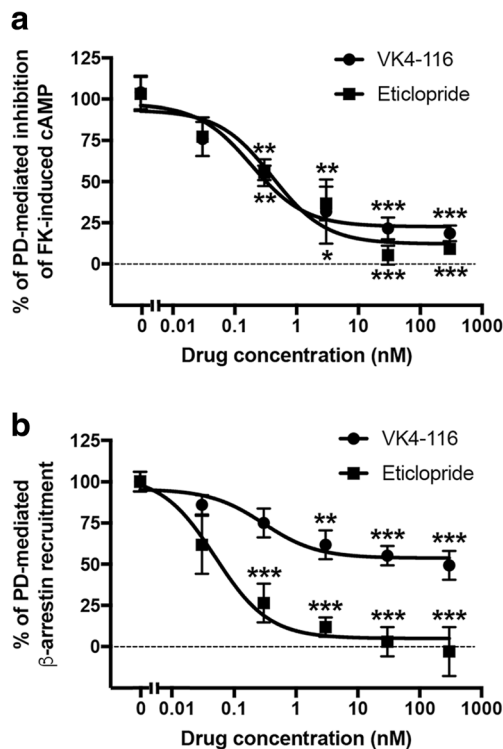
Fig. 4 Differential effect of the D3R antagonists VK4–116 and eticlopride on agonist-induced G protein-dependent signaling and β-arrestin-recruitment in D1R-D3R cells. Dose-response inhibition curves of the counteracting effect of VK4–116 and eticlopride on PD 128907 (PD)-mediated inhibition of forskolin-induced cAMP (**a**) and on PD 128907-mediated β-arrestin recruitment (**b**). For IC50 and Emax values, see "Results." In **a**, CHO cells were transfected with the cDNA corresponding to D1R-Rluc (1-μg cDNA) and D3R-YFP (1.5-μg cDNA). In 48 h post-transfection, D1R-D3R cells were treated for 10 min with vehicle or with the D3R antagonist VK4–116 or the D2-like receptor antagonist eticlopride (0.03–300 nM) before treatment for 7 min with medium or the D3R agonist PD 128907 (1 μM) in the presence of 0.5-μM forskolin (FK) for 15 min. In **b**, CHO cells were transfected with the cDNA corresponding to D3R-YFP (1-μg cDNA), β-arrestin-1-Rluc (0.5-μg cDNA), and D1R (1.5-μg cDNA). In 48 h post-transfection, cells were treated for 10 min with vehicle or VK4–116 or eticlopride (0.03–300 nM) before treatment with PD (1 μM) for 7 min, and β-arrestin-1 recruitment was measured by BRET (see "Material and Methods"). Values are mean ± S.E.M.; in **a**, $n = 4$ with duplicates; in **b**, $n = 7$ with duplicates; ** and *** $p < 0.001$ and $p < 0.0001$ versus in the absence of dopamine receptor antagonist (one-way ANOVA followed Newman-Keuls post hoc comparisons)

Fig. 5 Differential effect of the D3R antagonists VK4–116 and eticlopride on D1R-D3R agonist-induced locomotor activity in reserpinized mice. **a**, **b** Mice were administered reserpine (5 mg/kg, s.c.) 20 h before administration of the D1R agonist SKF 81297 (SKF; 5 mg/kg, i.p.), the D3R agonist PD 128907 (PD; 1 mg/kg, i.p.), or both, with or without previous administration (15 min before) of the D1R antagonist SCH 23390 (SCH; 0.5 mg/kg, i.p.), the D2-like receptor antagonist eticlopride (Etic; 0.1, 0.3, and 0.5 mg/kg, i.p.), or the D3R antagonist VK4–116 (VK; 30 and 100 mg/kg, i.p.). Values are mean ± S.E.M. ($n = 6$–10) and are expressed as the average of the transformed counts (squared root) obtained from the 10 min-periods recorded for 1 h. ** $p < 0.01$ versus SKF (one-way ANOVA followed by Newman-Keuls post hoc comparisons)

activation of post-synaptic D1R, while the synergistic locomotor activity induced by PD 128907 (1 mg/kg) plus SKF 81297 (5 mg/kg) could represent the simultaneous activation of post-synaptic D1R and D3R in the D1R-D3R heteromer. Assuming that functional D1R-D3R heteromers mediate the apparent synergistic locomotor activating effect of PD 128907 plus SKF 81297 and assuming that this synergistic effect depends on the G protein-independent signaling induced by co-activation of D1R and D3R in the D1R-D3R heteromer, eticlopride should be significantly more potent than VK4–116 at antagonizing the potentiating effect of PD 128907 on
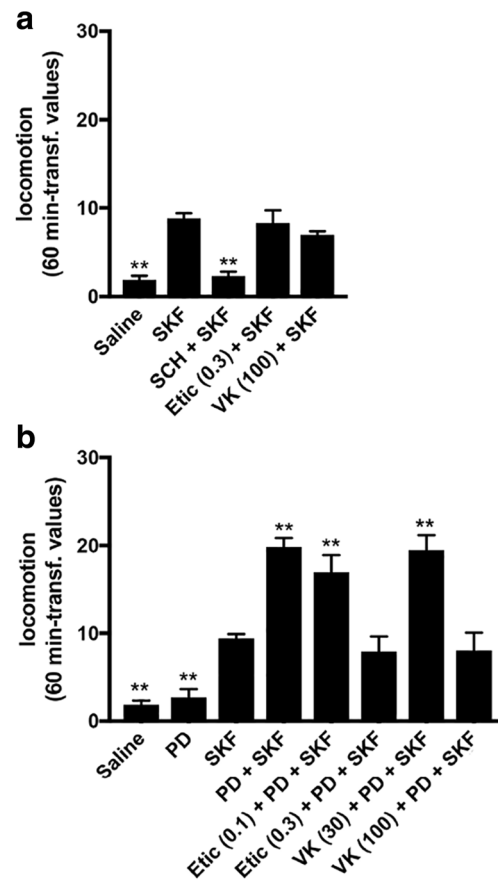
SKF 81297-mediated locomotor activation. In fact, the minimal doses of eticlopride and VK4–116 that were significantly effective were 0.3 and 100 mg/kg, respectively (Fig. 4b). This differential effect could be explained by the biased D3R antagonism of VK4–116 and agrees with a G protein-independent mechanism mediating the locomotion induced by D1R plus D3R activation in the D1R-D3R heteromer. These results, therefore, strongly support the existence of pharmacologically significant D1R-D3R heteromers in the striatum, which mediate the locomotor activating-effects induced by the simultaneous administration of D1R and D3R agonists in reserpinized mice.

We then looked for the two independent mechanisms of D1R-mediated MAPK activation demonstrated in transfected mammalian cells in the striatum of reserpinized mice. First,

we studied the ex vivo immunohistochemical analysis of striatal MAPK activation (ERK1/2 phosphorylation) in reserpinized mice after systemic administration of D1R and D3R agonists. As compared with vehicle-treated animals, ERK1/2 phosphorylation was not significantly modified by the administration of PD 128907 (1 mg/kg), but it was significantly increased upon SKF 81297 administration alone or in combination with PD 128907 (Fig. 6). Remarkably, in both cases, striatal MAPK activation was restricted to the most ventromedial part of the NAc, the shell of the NAc (Fig. 6), where D3R has been previously described to be preferentially expressed [1, 2]. Although there was a trend for a greater effect with combined treatment, different to the effects on locomotor activity, there were no significant differences between SKF 81297 alone or with PD 128907 and both groups showed a high inter-individual variability (see Fig. 7). These results would suggest that, in vivo, D3R activation does not produce MAPK activation on its own but promotes a switch from G protein-dependent to G protein-independent signaling
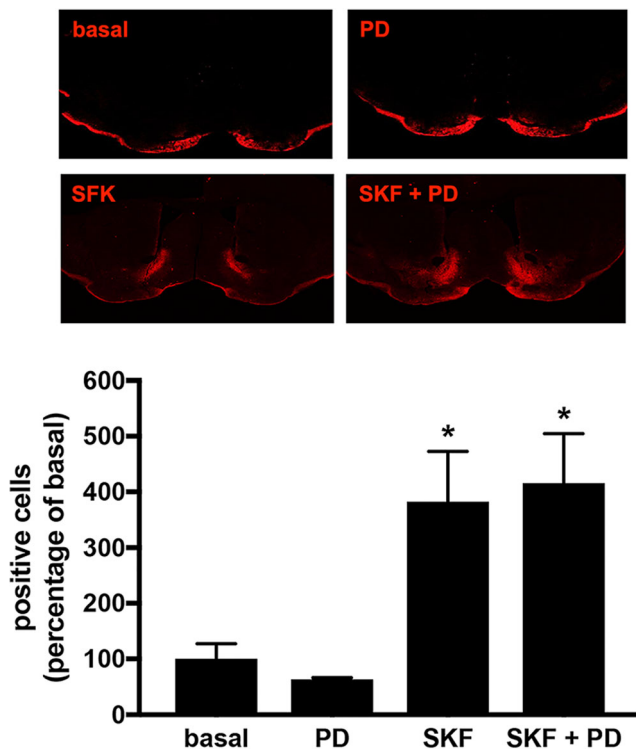

Fig. 6 ERK1/2 phosphorylation in the NAc of reserpinized mice induced by D1R and D3R agonists. Mice were administered reserpine (5 mg/kg, s.c.) 20 h before administration of the D1R agonist SKF 81297 (SKF; 5 mg/kg, i.p.), the D3R agonist PD 128907 (PD; 1 mg/kg, i.p.), or both. Twenty minutes after, mice were given an overdose of anesthetic and transcardially perfused (see "Material and Methods") to process the brains for the immunohistochemical analysis of ERK1/2 phosphorylation. Positive cells were counted within the area of the shell of the NAc of both sides from several coronal sections (from 2.28 to 1.44 mm anterior to bregma). Values are mean ± S.E.M. ($n = 6$–9) and are expressed as percentage of number of cells/mm^2 of the basal group (treated with saline); $* p < 0.05$ versus basal (one-way ANOVA followed Newman-Keuls post hoc comparisons)

of the D1R in the D1R-D3R heteromer. In fact, a significantly different biochemical profile of D1R agonist- versus D1R plus D3R agonist-dependent MAPK activation could be demonstrated using an intra-individual design, when comparing positive cells from both sides of the same brain slice from mice that received a unilateral infusion of a D1R-D3R heteromer-interfering peptide or the PKA inhibitor H-89 in the shell of the NAc. Although it might be argued that the experimental manipulation of the NAc contralateral and ipsilateral to the implanted infusion cannula is not even, the results obtained from the relative comparison of the effect of different treatments allowed establishing the validity of the values from the contralateral NAc as controls. This argument depends also on the previous demonstration of the specificity of the peptide approach in transfected cells, with TM5 of the D1R, but not TM7, specifically disrupting D1R-D3R heteromerization and the synergistic effect of D1R and D3R agonists on MAPK signaling [5]. On the other hand, it was also found that neither peptide modified MAPK activation induced by the sole administration of a D1R agonist. If the MAPK activation induced by the D1R agonist or by co-administration of D1R and D3R agonists in the NAc ipsilateral and contralateral to the implanted probe were experimentally comparable, we should only expect a significant difference (a decrease) in the effect of D1R plus D3R agonist in the ipsilateral striatum infused with TM5. In addition, no effect should be observed with TM7 and neither TM5 nor TM7 should modify the MAPK activation induced by the D1R agonist alone or with co-administration of the D3R agonist in the ipsilateral versus the contralateral NAc. These were in fact the results obtained, validating the values of the non-implanted contralateral NAc as control: Infusion of TM5 of D1R, but not the negative control TM7, significantly reduced ERK1/2 phosphorylation induced by co-administration of SKF 81297 and PD 128907, but it did not modify ERK1/2 phosphorylation induced by administration of SKF 81297 alone (Fig. 7a–d). On the other hand, infusion of H-89 significantly reduced ERK1/2 phosphorylation induced by administration of SKF 81297 alone, but it did not modify ERK1/2 phosphorylation induced by co-administration of SKF 81297 and PD 128907 (Fig. 7e–f). A paired t test was applied for statistical comparisons, which also allowed to control the substantial interindividual variability of ERK1/2 phosphorylation induced by the dopamine receptor agonists. Plots showing all the data and lines connecting the corresponding ipsilateral and contralateral values per animal are shown to disclose this variability (Fig. 7e–f).

Expression of D1R and D3R by q-PCR in the ventral striatum (which included both NAc core and shell) of reserpinized mice versus controls was also analyzed in order to evaluate the possibility of an upregulation of D1R-D3R heteromers upon reserpine-induced dopamine
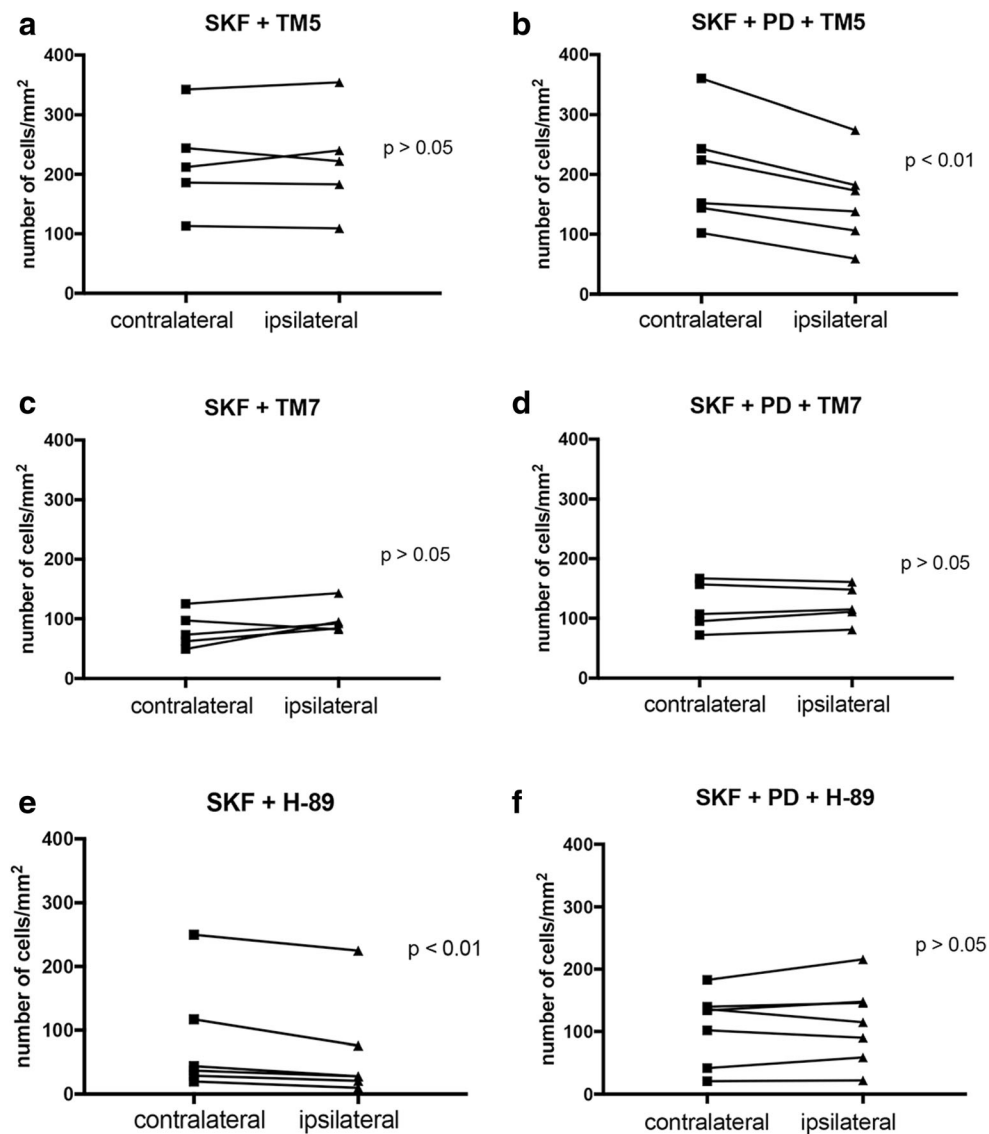
Fig. 7 Effect of the PKA inhibitor H-89 and D1R TAT-TM peptides on D1R-D3R agonist-induced striatal ERK1/2 phosphorylation in reserpinized mice. Mice were administered reserpine (5 mg/kg, s.c.) 20 h before administration of the D1R agonist SKF 81297 (SKF; 5 mg/kg, i.p.), alone (**a**, **c**, **e**), or co-administered with the D3R agonist PD 128907 (PD; 1 mg/kg, i.p.) (**b**, **d**, **f**). The agonists were administered 40 min after starting the intracerebral infusion of TAT-TM peptides (**a**–**d**) or the PKA inhibitor H-89 (**e**, **f**). After 60 min of intracranial infusion (20 min after the agonists administration), mice were given an overdose of anesthetic and transcardially perfused (see "Material and Methods") to process the brains for the immunohistochemical analysis of ERK1/2 phosphorylation. Positive cells were counted within the area of the shell of the NAc of both sides from several coronal sections immediate anterior to the cannula implantation (from 2.28 to 1.44 mm anterior to bregma) and, for each animal, values from the side ipsilateral to the intracerebral infusion was compared to the contralateral side. Values ($n = 6$–9) are expressed as number of cells/mm^2. p values represent the results of paired t test used to determine significant differences between the NAc ipsilateral to the intracranial infusion versus the contralateral side

depletion. The ratio of the expression of target/GADPH transcripts for D1R in reserpinized mice and controls (in mean ± S.E.M.) were 0.26 ± 0.02 and 0.30 ± 0.02, respectively; and for D3R, they were 0.009 ± 0.002 and 0.007 ± 0.002, respectively (non-paired Student' t test: $p > 0.05$ in both cases). Thus, D3R expression was about 30 times lower than D1R expression in the NAc, which was expected since the ventral striatal sample also included the core of the NAc, which expresses very low density of

D3R [1, 2]. D3R expression was almost undetectable in the dorsal striatum of either reserpinized mice or controls, again, without showing significant differences: target/GADPH transcripts values (in mean ± S.E.M.) were 0.00002 ± 0.00001 and 0.00003 ± 0.00001, respectively (non-paired Student' t test: $p > 0.05$). In summary, the results of q-PCR experiments showed no evidence for reserpine-induced up-regulation of D3R in either the ventral or the dorsal striatum.

Synergistic Effect of D1R and D3R Co-activation on AKT Phosphorylation in D1R-D3R Transfected Cells and in Reserpinized Mice

The lack of synergistic effect on MAPK activation upon co-activation of D1R and D3R in the NAc implies that striatal MAPK activation cannot be a main determinant of the synergistic locomotor activation induced by D1R and D3R agonists. Nevertheless, MAPK activation is one of the various G protein-independent, β-arrestin-dependent, downstream signaling pathways of D_2-like receptors with behavioral significance, which also includes the Akt/GSK3 signaling pathway [26, 27]. Therefore, we aimed first at evaluating the possible existence of a synergistic effect of D1R and D3R agonists on AKT phosphorylation in reserpinized mice. Using the same doses from prior experiments, neither PD 128907 nor SKF 81297 produced a significant AKT phosphorylation in the NAc as compared to vehicle-treated mice (Fig. 8). Nevertheless, co-administration of the D1R and D3R agonists led to a significant and selective increase within the same ventral striatal area that showed MAPK activation upon administration of SKF 81297 alone or with PD 128907 (Fig. 8). AKT phosphorylation was then analyzed in CHO cells transfected with both D1R and D3R. As expected, PD 128907, but not SKF 81297, produced a significant increase in AKT phosphorylation, in agreement with their respective ability to promote G protein-independent and G protein-dependent signaling in D1R-D3R transfected cells (Fig. 9). Also, as expected, simultaneous administration of both compounds produced a significant synergistic effect (Fig. 9).
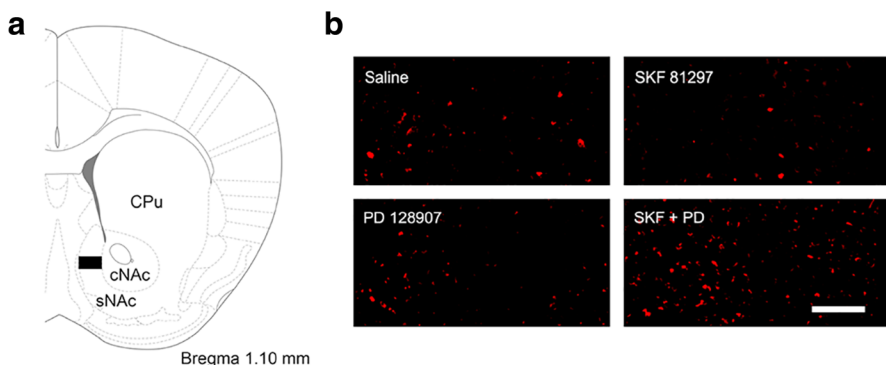
Fig. 9 Synergistic effect of D1R and D3R agonists on AKT phosphorylation in D1R-D3R cells. AKT phosphorylation in CHO cells transfected with D1R-Rluc (1 μg cDNA) and D3R-YFP (1.3 μg cDNA). 48 h post-transfection, cells were treated for 7 min with the D1R agonist SKF 38393 (1 μM), the D3R agonist PD 128907 (1 μM) or both. Quantification of phosphorylated AKT was determined by Western blot. Representative blots are shown. Values are mean ± S.E.M. ($n = 4$ with duplicates) and are expressed as percentage of basal, non-treated cells; * and *** $p < 0.05$ and $p < 0.001$ versus basal, respectively (one-way ANOVA followed by Newman-Keuls post hoc comparisons)

Discussion

The present study demonstrates the presence of pharmacologically significant D1R-D3R heteromers in the mouse ventromedial striatum, the shell of the NAc, with very similar

Fig. 8 Synergistic effect of D1R and D3R agonists on AKT phosphorylation in the NAc. Mice were administered reserpine (5 mg/kg, s.c.) 20 h before administration of the D1R agonist SKF 81297 (5 mg/kg, i.p.), the D3R agonist PD 128907 (1 mg/kg, i.p.), or both. Twenty minutes after, mice were given an overdose of anesthetic and transcardially perfused (see "Material and Methods") to process the brains for the immunohistochemical analysis of AKT phosphorylation. Positives cells were counted within the area of the shell of the NAc of both sides from several coronal sections (around 1.10 mm anterior to
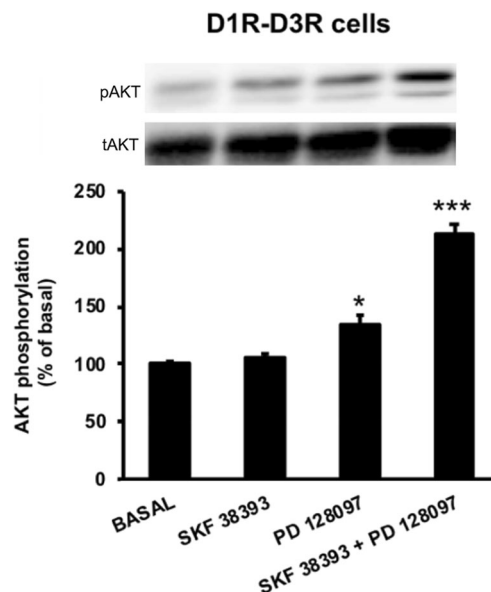
bregma). In **a**, scheme a of a coronal mouse brain section indicating the localization (black rectangle) of the mages shown in **b**, which are representative images of the four experimental conditions, saline, SKF 81297, PD 128907, and SKF 81297 + PD 128907 (SKF + PD); scale bar: 0.1 mm. In **c**, values are mean ± S.E.M. ($n = 6$–9) and are expressed as number of cells/mm^2; *** $p < 0.001$ versus saline (one-way ANOVA followed Newman-Keuls post hoc comparisons). CPu, cNAc, and sNAc: caudate-putamen, core and shell of the NAc, respectively

biochemical characteristics than the D1R-D3R analyzed in mammalian transfected cells. D1R and D3R are respectively coupled to Gs and Gi in transfected cells, where synthetic TM peptides that destabilize the D1R-D3R heteromeric interface block the D3R-mediated counteraction of cAMP formation induced by D1R activation. This implies that D1R-D3R heteromers can be included in the recently proposed class of Gs-Gi-coupled heterotetramers [28], which provide the framework for the simultaneous intermolecular interactions that allow the canonical Gs-Gi antagonistic interaction at the AC level [17, 18]. The results of the present study further indicate that, in the D1R-D3R heteromer, D1R activates MAPK solely through the Gs-AC-PKA-dependent signaling, while D3R coactivation leads to a shift in D1R signaling, from a G protein-dependent mechanism (which is blocked by the canonical interaction at the AC level) to a G protein-independent mechanism, which includes MAPK and AKT activation (Fig. 10). In situ application of TM peptides and a PKA inhibitor confirmed the existence of the two D1R-D3R heteromer-dependent mechanisms of D1R-mediated activation of MAPK in the NAc of reserpinized mice.

Numerous examples of G protein-dependent signaling and G protein-independent (often, ß-arrestin-dependent) signaling by the same receptor have been reported. At the same time,
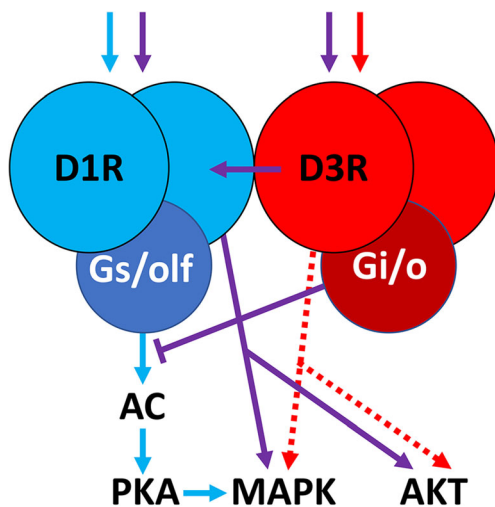

Fig. 10 Scheme of the switch of G protein-dependent to G protein-independent signaling of D1R upon co-activation of D3R within the D1R-D3R heterotetramer. Both in mammalian transfected cells and in the shell of the NAc, selective activation of the D1R leads to a Gs/olf-dependent activation of MAPK activation secondary to adenylyl cyclase (AC) and PKA activation (blue arrows). In transfected cells, but not in the NAc, activation of the D3R leads to a G protein-independent and probably ß-arrestin-dependent activation of MAPK and phosphorylation of AKT (solid and broken red arrows). Both, in the NAc and in transfected cells, coactivation of D1R and D3R in the D1R-D3R heterotetramer leads to a Gi/o-Gs/olf canonical interaction with AC inhibition and to a significant G protein-independent (and probably ß-arrestin-dependent) MAPK and AKT activation (purple arrows). G protein-independent signaling by the D1R-D3R heteromer correlates with the synergistic locomotor activation of D1R and D3R agonists in reserpinized mice

"biased signaling" or "functional selectivity," the ability of a ligand to selectively activate (biased agonist) or block (biased antagonist) G protein-dependent or independent signaling, has become a main quest in GPCR pharmacology [29–32]. Previous studies have already indicated that receptor heteromerization can promote functional selectivity, such as the ability of µ-opioid receptor activation to induce ß-arrestin-dependent MAPK activation upon heteromerization with the σ-opioid receptor [33]. Another example is the recent demonstration of D2R-mediated ß-arrestin2 recruitment upon heteromerization with the adenosine A_{2A} receptor [34]. The present study extends these findings with, to our knowledge, the first example where a biased signaling (D1R-mediated, G protein-independent MAPK activation) is determined by co-activation of a partner receptor (D3R) in a GPCR heteromer (D1R-D3R heteromer).

Since D1R expression is homogeneously distributed in all striatal areas, it was first surprising to observe that isolated systemic administration of a D1R agonist selectively induces MAPK activation in the shell of the NAc. Nevertheless, the same discrete MAPK activation in the ventromedial striatum had been previously observed by Gerfen and coworkers upon systemic administration of D1R agonists and upon endogenous dopamine release (by electrical activation of mesencephalic striatal dopaminergic afferents) [35]. Significantly, they also demonstrated that the pattern of D1R agonist-mediated MAPK extended to the whole striatum upon 6-hydroxydopamine-induced striatal dopamine denervation [35]. The authors concluded that D1R supersensitivity induced by prolonged dopamine denervation is related to a switch in MAPK signaling, with an extension of D1R agonist-induced MAPK activation from the ventral to the dorsal striatum [35]. Based on the present results, a very plausible mechanistic explanation for these findings is that D1R supersensitivity is dependent on an upregulation of D3R and an increase in D1R-D3R heteromer expression in dorsal striatal areas. In fact, an elegant electrophysiological study by Prieto and coworkers demonstrated that prolonged striatal dopamine depletion is associated with a selective supersensitivity of D3R, without changes in the other D2-like receptors D2R and D4R, which would occur not only in the D1R-expressing striatonigral but also in the D2R-expressing striatopallidal neurons [36].

It is well established that D3R upregulation within the dorsal striatum develops when dopamine depletion is associated with administration of non-selective dopamine receptor agonists, including L-DOPA treatment or selective D1R agonists [7, 37, 38], which should be associated with an increased expression of D1R-D3R heteromers [7, 8]. D3R upregulation and the concomitant D1R supersensitivity are currently viewed as a main pathogenetic mechanism of L-DOPA-induced dyskinesia [7–9, 37, 38]. Although the reserpinized mouse model used in the present study does not imply a

prolonged dopamine depletion (20 h) and is not associated with upregulation of D3R (qPCR experiments), the synergistic locomotor activity induced by D1R and D3R agonists in reserpinized mice can provide a valuable proxy model to study the mechanisms of L-DOPA-induced dyskinesia and to evaluate new therapeutic agents. First, we were able to establish that D1R-D3R co-activation in the D1R-D3R heteromer mediates the synergistic locomotor activity of D1R and D3R agonists in reserpinized mice. Second, we established that the biochemical mechanism involves a switch of D1R signaling, from G protein-dependent to G protein-independent signaling. Importantly, the biochemical finding that correlated with the behavioral D1R-D3R-mediated synergistic effect was striatal AKT phosphorylation, which is a G protein-independent and often β-arrestin-dependent signaling, previously shown to be selectively increased in L-DOPA-treated rats with prolonged striatal dopamine depletion and in MPTP-lesioned monkeys that develop L-DOPA-induced dyskinesia [39, 40].

Our results predict that a functionally selective D3R antagonist, with predominant blockade of ß-arrestin-dependent signaling, can be an efficacious treatment for L-DOPA-induced dyskinesia. In the present study, a selective D3R antagonist, VK4–116, showed the opposite profile, a biased antagonism for G protein-dependent versus G protein-independent signaling, which correlated with the need for high doses to counteract the synergistic locomotor-activating effect of D1R and D3R agonists in reserpinized mice. However, to our knowledge, no D3R-selective β-arrestin biased antagonist exists to further test our hypothesis. Selective D3R antagonists with higher potency for G protein-independent signaling could also be useful in other neuropsychiatric disorders where there is also evidence for D3R upregulation. For example, striatal D3R upregulation has also been found in human cocaine fatalities [41]. Thus, our study indicates that D1R-D3R heteromers should be considered as pharmacological targets for the treatment of L-DOPA-induced dyskinesia and for substance use disorders.

References

1. Schwartz JC, Diaz J, Bordet R, Griffon N, Perachon S, Pilon C, Ridray S, Sokoloff P (1998) Functional implications of multiple dopamine receptor subtypes: the D1/D3 receptor coexistence. Brain Res Rev 26:236–242

2. Sokoloff P, Giros B, Martres MP, Bouthenet ML, Schwartz JC (1990) Molecular cloning and characterization of a novel dopamine receptor (D3) as a target for neuroleptics. Nature 347:146–151

3. Ridray S, Griffon N, Mignon V, Souil E, Carboni S, Diaz J, Schwartz JC, Sokoloff P (1998) Coexpression of dopamine D1 and D3 receptors in islands of Calleja and shell of nucleus accumbens of the rat: opposite and synergistic functional interactions. Eur J Neurosci 10:1676–1686

4. Fiorentini C, Busi C, Gorruso E, Gotti C, Spano P, Missale C (2008) Reciprocal regulation of dopamine D1 and D3 receptor function and trafficking by heterodimerization. Mol Pharmacol 74:59–69

5. Guitart X, Navarro G, Moreno E, Yano H, Cai NS, Sánchez-Soto M, Kumar-Barodia S, Naidu YT et al (2014) Functional selectivity of allosteric interactions within G protein-coupled receptor oligomers: the dopamine D1-D3 receptor heterotetramer. Mol Pharmacol 86:417–429

6. Marcellino D, Ferré S, Casadó V, Cortés A, Le Foll B, Mazzola C, Drago F, Saur O et al (2008) Identification of dopamine D1-D3 receptor heteromers. Indications for a role of synergistic D1-D3 receptor interactions in the striatum. J Biol Chem 283:26016–26025

7. Farré D, Muñoz A, Moreno E, Reyes-Resina I, Canet-Pons J, Dopeso-Reyes IG, Rico AJ, Lluís C et al (2015) Stronger dopamine D1 receptor-mediated neurotransmission in dyskinesia. Mol Neurobiol 52:1408–1420

8. Ferré S, Lluis C, Lanciego JL, Franco R (2010) Prime time for G-protein-coupled receptor heteromers as therapeutic targets for CNS disorders: the dopamine D1-D3 receptor heteromer. CNS Neurol Disord Drug Targets 9:596–600

9. Lanza K, Meadows SM, Chambers NE, Nuss E, Deak MM, Ferré S, Bishop C (2018) Behavioral and cellular dopamine D(1) and D(3) receptor-mediated synergy: implications for L-DOPA-induced dyskinesia. Neuropharmacology 138:304–314

10. Ferré S, Giménez-Llort L, Artigas F, Martínez E (1994) Motor activation in short-and long-term reserpinized mice: role of N-methyl-D-aspartate, dopamine D1 and dopamine D2 receptors. Eur J Pharmacol 255:203–213

11. Starr BS, Starr MS, Kilpatrick IC (1987) Behavioural role of dopamine D1 receptors in the reserpine-treated mouse. Neuroscience 22:179–188

12. Missale C, Nash SR, Robinson SW, Jaber M, Caron MG (1998) Dopamine receptors: from structure to function. Physiol Rev 78:189–225

13. Gilman AG (1987) G proteins: transducers of receptor-generated signals. Annu Rev Biochem 56:615–649

14. Carriba P, Navarro G, Ciruela F, Ferré S, Casadó V, Agnati L, Cortés A, Mallol J et al (2008) Detection of heteromerization of more than two proteins by sequential BRET-FRET. Nat Methods 5:727–733

15. Bonaventura J, Navarro G, Casadó-Anguera V, Azdad K, Rea W, Moreno E, Brugarolas M, Mallol J et al (2015) Allosteric interactions between agonists and antagonists within the adenosine A2A receptor-dopamine D2 receptor heterotetramer. Proc Natl Acad Sci U S A 112:E3609–E3618

16. He SQ, Zhang ZN, Guan JS, Liu HR, Zhao B, Wang HB, Li Q, Yang H et al (2011) Facilitation of μ-opioid receptor activity by preventing δ-opioid receptor-mediated codegradation. Neuron 69:120–131

17. Navarro G, Cordomí A, Casadó-Anguera V, Moreno E, Cai NS, Cortés A, Canela EI, Dessauer CW et al (2018) Evidence for functional pre-coupled complexes of receptor heteromers and adenylyl cyclase. Nat Commun 9:1242

18. Rivera-Oliver M, Moreno E, Álvarez-Bagnarol Y, Ayala-Santiago C, Cruz-Reyes N, Molina-Castro GC, Clemens S, Canela EI et al (2018) Adenosine A(1)-dopamine D(1) receptor heteromers control

the excitability of the spinal motoneuron. Mol Neurobiol 56:797–811

19. Schwarze SR, Ho A, Vocero-Akbani A, Dowdy SF (1999) In vivo protein transduction: delivery of a biologically active protein into the mouse. Science 285:1569–1572

20. Kumar V, Bonifazi A, Ellenberger MP, Keck TM, Pommier E, Rais R, Slusher BS, Gardner E et al (2016) Highly selective dopamine D3 receptor (D3R) antagonists and partial agonists based on eticlopride and the D3R crystal structure: new leads for opioid dependence treatment. J Med Chem 59:7634–7650

21. Yano H, Cai NS, Xu M, Verma RK, Rea W, Hoffman AF, Shi L, Javitch JA et al (2018) Gs- versus Golf-dependent functional selectivity mediated by the dopamine D(1) receptor. Nat Commun 9:486

22. Andén NE, Grabowska-Andén M (1988) Stimulation of D1 dopamine receptors reveals direct effects of the preferential dopamine autoreceptor agonist B-HT 920 on postsynaptic dopamine receptors. Acta Physiol Scand 134:285–290

23. Chen J, Rusnak M, Lombroso PJ, Sidhu A (2009) Dopamine promotes striatal neuronal apoptotic death via ERK signaling cascades. Eur J Neurosci 29:287–306

24. Robinson SW, Jarvie KR, Caron MG (1994) High affinity agonist binding to the dopamine D3 receptor: chimeric receptors delineate a role for intracellular domains. Mol Pharmacol 46:352–356

25. Keck TM, John WS, Czoty PW, Nader MA, Newman AH (2015) Identifying medication targets for psychostimulant addiction: Unraveling the dopamine D3 receptor hypothesis. J Med Chem 58:5361–5380

26. Beaulieu JM, Tirotta E, Sotnikova TD, Masri B, Salahpour A, Gainetdinov RR, Borrelli E, Caron MG (2007) Regulation of Akt signaling by D2 and D3 dopamine receptors in vivo. J Neurosci 27:881–885

27. Salles MJ, Hervé D, Rivet JM, Longueville S, Millan MJ, Girault JA, Mannoury la Cour C (2013) Transient and rapid activation of Akt/GSK-3β and mTORC1 signaling by D3 dopamine receptor stimulation in dorsal striatum and nucleus accumbens. J Neurochem 125:532–544

28. Ferré S (2015) The GPCR heterotetramer: challenging classical pharmacology. Trends Pharmacol Sci 36:145–152

29. Costa-Neto CM, Parreiras-E-Silva LT, Bouvier M (2016) Pluridimensional view of biased agonism. Mol Pharmacol 90:587–595

30. Reiter E, Ahn S, Shukla AK, Lefkowitz RJ (2012) Molecular mechanism of β-arrestin-biased agonism at seven-transmembrane receptors. Annu Rev Pharmacol Toxicol 52:179–197

31. Urs NM, Peterson SM, Caron MG (2017) New concepts in dopamine D(2) receptor biased signaling and implications for schizophrenia therapy. Biol Psychiatry 81:78–85

32. Violin JD, Crombie AL, Soergel DG, Lark MW (2014) Biased ligands at G-protein-coupled receptors: promise and progress. Trends Pharmacol Sci 35:308–316

33. Rozenfeld R, Devi LA (2007) Receptor heterodimerization leads to a switch in signaling: beta-arrestin2-mediated ERK activation by mu-delta opioid receptor heterodimers. FASEB J 21:2455–2465

34. Sahlholm K, Gómez-Soler M, Valle-León M, López-Cano M, Taura JJ, Ciruela F, Fernández-Dueñas V (2018) Antipsychotic-like efficacy of dopamine D(2) receptor-biased ligands is dependent on adenosine A(2A) receptor expression. Mol Neurobiol 55:4952–4958

35. Gerfen CR, Miyachi S, Paletzki R, Brown P (2002) D1 dopamine receptor supersensitivity in the dopamine-depleted striatum results from a switch in the regulation of ERK1/2/MAP kinase. J Neurosci 22:5042–5054

36. Prieto GA, Perez-Burgos A, Palomero-Rivero M, Galarraga E, Drucker-Colin R, Bargas J (2011) Upregulation of D2-class signaling in dopamine-denervated striatum is in part mediated by D3 receptors acting on Ca V 2.1 channels via PIP2 depletion. J Neurophysiol 105:2260–2274

37. Bordet R, Ridray S, Carboni S, Diaz J, Sokoloff P, Schwartz JC (1997) Induction of dopamine D3 receptor expression as a mechanism of behavioral sensitization to levodopa. Proc Natl Acad Sci U S A 94:3363–3367

38. Solís O, Garcia-Montes JR, González-Granillo A, Xu M, Moratalla R (2017) Dopamine D3 receptor modulates l-DOPA-induced dyskinesia by targeting D1 receptor-mediated striatal signaling. Cereb Cortex 27:435–446

39. Bychkov E, Ahmed MR, Dalby KN, Gurevich EV (2007) Dopamine depletion and subsequent treatment with L-DOPA, but not the long-lived dopamine agonist pergolide, enhances activity of the Akt pathway in the rat striatum. J Neurochem 102:699–711

40. Morissette M, Samadi P, Hadj Tahar A, Bélanger N, Di Paolo T (2010) Striatal Akt/GSK3 signaling pathway in the development of L-Dopa-induced dyskinesias in MPTP monkeys. Prog Neuro-Psychopharmacol Biol Psychiatry 34:446–454

41. Staley JK, Mash DC (1996) Adaptive increase in D3 dopamine receptors in the brain reward circuits of human cocaine fatalities. J Neurosci 16:6100–6106

Publisher's Note Springer Nature remains neutral with regard to jurisdictional claims in published maps and institutional affiliations.